AMERICAN ACADEMY OF OPHTHALMOLOGY®

Epiretinal Membrane Impairs the Inner Retinal Layer in a Traction Force-Dependent Manner

Yuki Kanzaki, MD, PhD,[1] *Ryo Matoba, MD, PhD,*[1] *Shuhei Kimura, MD, PhD,*[1] *Mio M. Hosokawa, MD, PhD,*[1] *Yusuke Shiode, MD, PhD,*[1] *Shinichiro Doi, MD, PhD,*[1] *Tetsuro Morita, MD,*[1] *Sayumi Kanzaki, MD,*[1] *Ippei Takasu, MD, PhD,*[2] *Atsuhiro Tanikawa, MD, PhD,*[3] *Yuki Morizane, MD, PhD*[1]

Purpose: To investigate the relationship between retinal traction force and impairment of the inner retinal layer in patients with epiretinal membrane (ERM).

Design: Nonrandomized, retrospective consecutive case series.

Participants: Two hundred nine eyes of 201 patients with idiopathic ERM who underwent vitrectomy for idiopathic ERM were enrolled.

Methods: Retinal folds caused by ERM were visualized using en face OCT, and the maximum depth of retinal folds within the parafovea (MDRF) was measured. Focal macular electroretinogram (ERG) was used to measure the amplitude and implicit time of each component for the ERM eyes and the normal fellow eyes. B-scan OCT images were used to measure the thicknesses of the inner nuclear layer (INL) and outer nuclear layer (ONL) + outer plexiform layer (OPL). Expression of α-smooth muscle actin (α-SMA) in surgically removed ERM specimens was quantified by reverse-transcription polymerase chain reaction.

Main Outcome Measures: We analyzed the relationship between MDRF and the relative amplitudes of focal macular ERG (affected eye/fellow eye), the relationships between MDRF and the mean INL thickness and ONL+OPL thickness, comparison of INL thickness and ONL+OPL thickness for each area when cases were classified according to MDRF localization in the ETDRS chart, and the relationship between MDRF and the relative expression of α-SMA in the ERM specimens.

Results: The MDRF significantly correlated with the relative amplitudes (affected eye/fellow eye) of b-waves and oscillatory potentials ($r = -0.657$, $P = 0.015$; $r = -0.569$, $P = 0.042$, respectively) and the mean INL thickness and ONL+OPL thickness ($r = 0.604$, $P < 0.001$; $r = 0.210$, $P = 0.007$, respectively). However, only the INL thickness progression rate was significantly correlated with the MDRF progression rate ($r = 0.770$, $P < 0.001$). On case stratification by localization of MDRF based on the ETDRS chart, in regions other than temporal regions, the INL thickness was significantly greater in regions with MDRF than in other regions. The MDRF significantly correlated with α-SMA expression in the ERM specimens ($r = 0.555$, $P = 0.009$).

Conclusions: The findings suggest that ERM impairs the inner retinal layer in a traction force-dependent manner.

Financial Disclosure(s): The author(s) have no proprietary or commercial interest in any materials discussed in this article. *Ophthalmology Science 2023;3:100312*

Supplemental material available at www.ophthalmologyscience.org.

Introduction

Epiretinal membrane (ERM) is a common type of fibrocellular proliferation found on the internal limiting membrane (ILM), and is significantly associated with aging.[1–3] The major symptoms of ERM include reduced visual acuity, metamorphopsia, and aniseikonia.[4–10] However, the pathophysiological mechanisms underlying the onset of these symptoms remain unclear.

Among the various symptoms of ERM, metamorphopsia is the most important because it appears the earliest[11] and affects quality of vision the most.[5,11] The relationship between metamorphopsia and changes in the retinal structure has been investigated using high-resolution OCT images.[4,6,7,12,13] As a result, it has been reported that the thicknesses of specific retinal layers are strongly correlated with the score in M-CHARTS, a subjective quantitative test for metamorphopsia.[4,6,7,13] For example, thickening of the inner

https://doi.org/10.1016/j.xops.2023.100312
ISSN 2666-9145/23

nuclear layer (INL) and appearance of an ectopic inner foveal layer were reportedly observed with ERM progression.[14] However, the mechanism by which ERM causes changes in the thicknesses of specific retinal layers remains unknown.

Tangential retinal traction force applied by ERM has been considered an important mechanism for metamorphopsia and changes in the thicknesses of specific retinal layers.[6,7,13,15] However, it has been difficult to elucidate the role of retinal traction force in the pathophysiology of ERM because there was no means to objectively and quantitatively assess the retinal traction force. Recently, we focused on the depth of retinal folds caused by ERM and reported that this depth is an important objective and quantitative biomarker reflecting the tangential retinal traction force applied by ERM.[12,16–20] We further examined the relationship between the preoperative maximum depth of retinal folds within the parafovea (MDRF) and metamorphopsia and found that MDRF was significantly related to preoperative metamorphopsia.[16,19,21] In addition, utilizing the relationship between MDRF and metamorphopsia, we quantitatively identified the optimal timing of ERM surgery that does not compromise the patient's quality of life.[19]

In the present study, with the aim of clarifying the effects of retinal traction force by ERM on each retinal layer, we investigated the relationships between MDRF and (1) changes in the electrophysiological response of the retina, (2) changes in the INL and outer nuclear layer

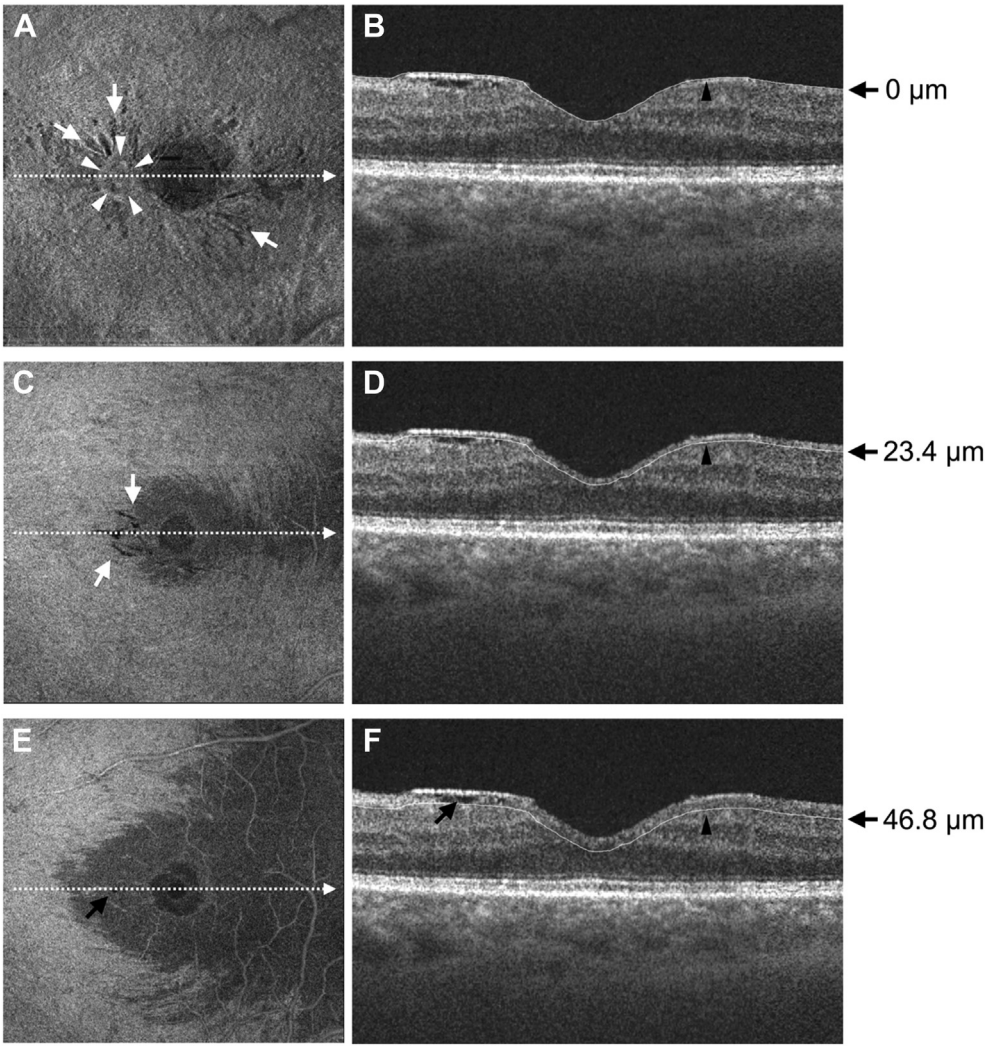

Figure 1. Measurement of the maximum depth of retinal folds (MDRF) using en face images of patients with epiretinal membrane (ERM). En face OCT images (**A, C,** and **E**) and B-scan OCT images (**B, D,** and **F**) at the level of the internal limiting membrane (ILM) (**A, B**), 23.4 μm below the ILM level (**C, D**), and 46.8 μm below the ILM level (**E, F**) are shown. The white line (black arrowhead in **B, D,** and **F**) indicates the depth at which the en face OCT images (**A, C,** and **E**) were constructed. The white dotted line (**A, C,** and **E**) indicates the scan section of the B-scan images in **B, D,** and **F**. The white arrowheads (**A**) indicate ERM. The white arrows indicate the retinal folds caused by retinal traction due to ERM (**A, C**). The black arrow (**E, F**) indicates the deepest retinal fold in the parafoveal area. The deepest retinal fold disappeared in the en face OCT image constructed at a level deeper than that in this image (**E**). Therefore, MDRF in this case was 46.8 μm.

(ONL) + outer plexiform layer (OPL) thicknesses, and (3) the expression of proteins in ERM that are related to the retinal traction force.

Methods

Study Design and Subjects

This study was a nonrandomized, retrospective consecutive case series. The study protocol was approved by the Ethics Committee of Okayama University Hospital, Okayama, Japan (K2205-010 and K1608-014) and adhered to the tenets of the Declaration of Helsinki. Two hundred nine eyes of 201 patients with idiopathic ERM who underwent vitrectomy for idiopathic ERM from June 1, 2016 through November 30, 2021 at Okayama University Hospital or Takasu Eye Clinic were enrolled. After surgery, the specimens were used for immunohistological staining and real-time reverse transcription polymerase chain reaction as described later. We excluded eyes with secondary ERM associated with ocular diseases such as age-related macular degeneration, diabetic retinopathy, and retinal vein occlusion. Each patient was informed about the nature and possible consequences of the study and provided written informed consent for participation.

Ophthalmic Examinations

All patients underwent comprehensive ophthalmic examinations, including assessments using slit-lamp biomicroscopy and swept-source OCT (Triton; Topcon Corporation). M-CHARTS (Inami) were used to quantify the degree of metamorphopsia.[21] The M-CHARTS score was obtained by examining M-CHARTS for the vertical and horizontal directions and calculating the average of the values.[6,7,19]

Analysis of Swept-Source OCT Images

Swept-source OCT images were obtained in both B-scan and 3-dimensional modes (7 × 7-mm area, 512 × 512 A-scans). Image analysis software (IMAGEnet6, Version 1.22 software, Topcon Corporation) was used to construct en face images.

Measurement of MDRF

We measured MDRF within a 3-mm-diameter circle centered at the fovea (parafoveal area in the ETDRS chart) as previously described.[12,16–19] Briefly, we flattened the 3-dimensional OCT volume scan data at the level of ILM and visualized the black lines corresponding to the retinal folds due to retinal traction by ERM on the en face image below the ILM level. Then, we measured the depth from ILM just before the deepest retinal fold within the parafoveal area disappeared (Fig 1).

Measurement of Focal Macular Electroretinogram

Focal macular electroretinogram (ERG) was performed using ER-80 (Kowa) according to the method of previous reports (Supplementary Method).[22–24] For statistical analysis, the amplitude of each component for the ERM eye was calculated with the amplitude of each component for the normal fellow eye set as 1 (called the relative amplitude). The relationships between MDRF and the relative amplitudes of a- and b- waves and oscillatory potentials (OPs) were analyzed.

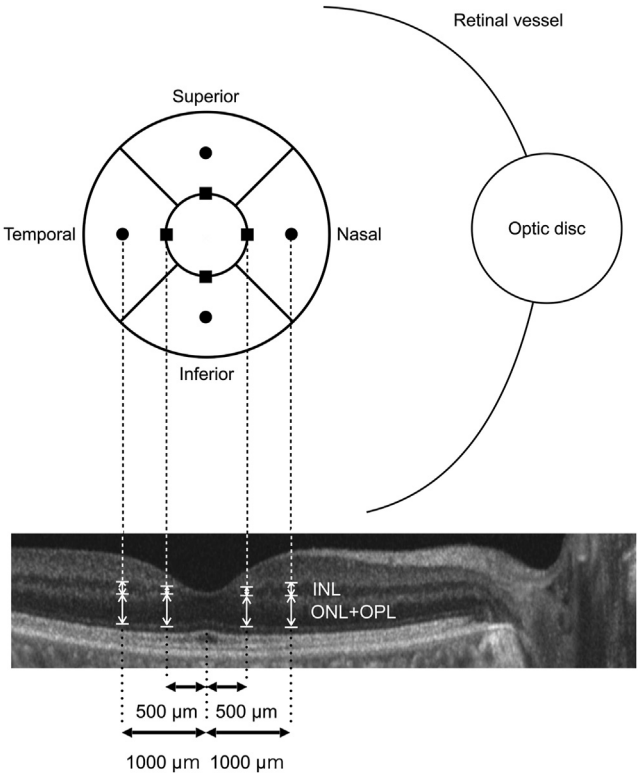

Figure 2. Measurement of the retinal layer thickness on B-scan OCT images of patients with epiretinal membrane. The inner nuclear layer (INL) and outer nuclear layer (ONL) + outer plexiform layer (OPL) thicknesses are measured at a total of 8 points that are 500 μm (black squares) and 1000 μm (black circles) superior, inferior, nasal, and temporal to the fovea. The thicknesses at the 4 points that are 500 μm superior, inferior, nasal, and temporal to the fovea are used to calculate the mean INL and ONL+OPL thicknesses. The 4 points that are 1000 μm away from the fovea are used to indicate the thickness of the center of each area on the ETDRS chart.

Measurement of the Mean INL and ONL+OPL Thicknesses

B-scan OCT images in vertical and horizontal cross-sections through the fovea were used to measure the INL and ONL+OPL thicknesses. Measurements were obtained from points located 500 μm and 1000 μm away from the fovea in the superior, inferior, nasal, and temporal regions (1 point at 500 μm and 1 at 1000 μm in each of the 4 regions; total 8 points)[6,7] (Fig 2). The mean INL and ONL+OPL thicknesses were defined as the average of the INL and ONL+OPL thicknesses at the 4 points located 500 μm from the fovea (superior, inferior, nasal, and temporal regions). The INL and ONL+OPL thicknesses at the 4 points located 1000 μm away from the fovea were used to indicate the thickness of each region on the ETDRS chart (Fig 2).

Quantification of the Progression Rates for MDRF and the Mean INL and ONL+OPL Thicknesses Over the Natural Course of ERM

We measured MDRF and the mean INL and ONL+OPL thicknesses at 2 time points ≥ 6 months apart in patients who were followed up without ERM surgery. The progression rates for

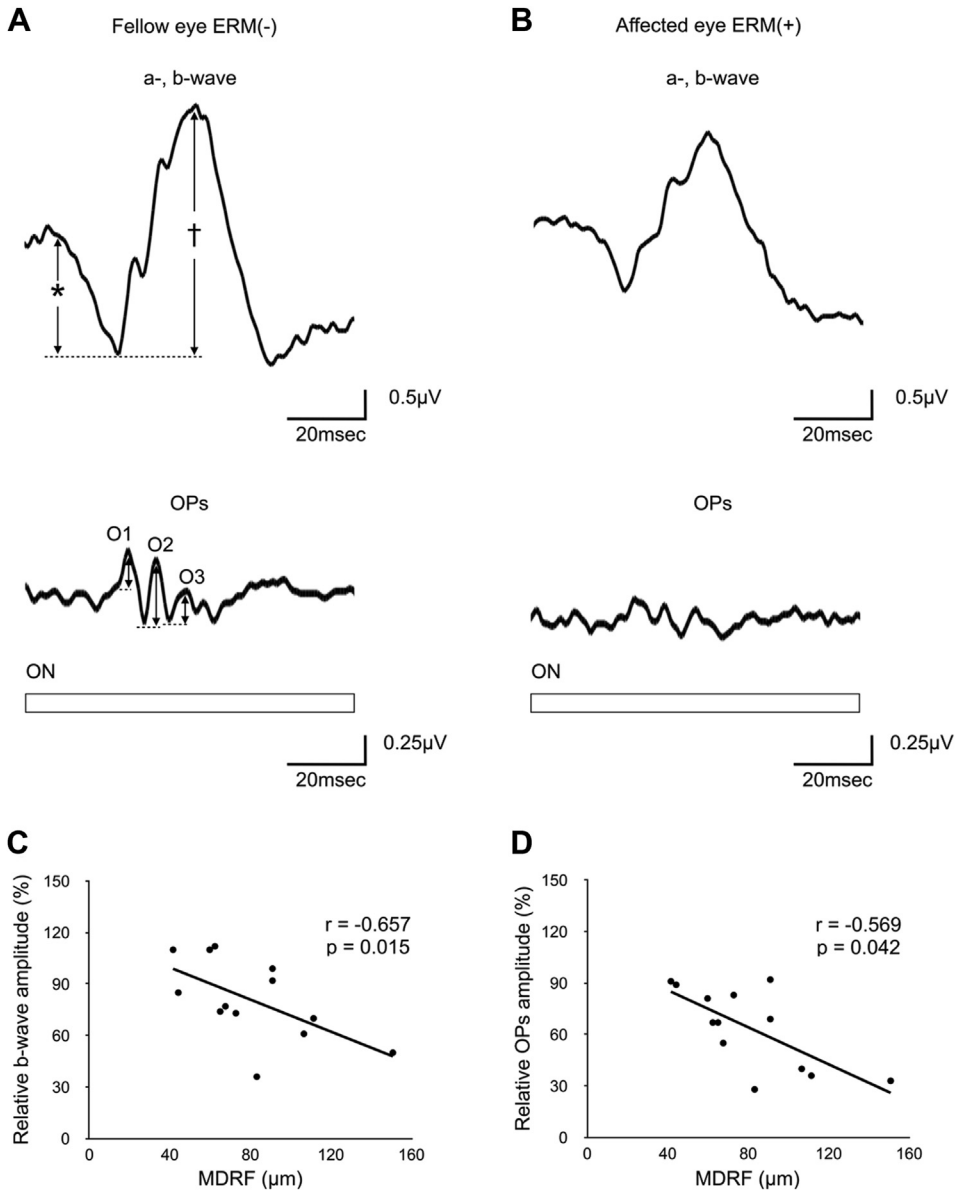

Figure 3. Relationships between the maximum depth of retinal folds (MDRF) and each component of focal macular electroretinogram (fmERG) in a representative case involving a 71-year-old woman with epiretinal membrane (ERM). **A, B,** fmERG components for the normal fellow eye (**A**) and the affected eye with ERM (**B**) are shown. **C, D,** Relationships between MDRF and relative amplitudes (affected eye/fellow eye) of b-waves and oscillatory potentials (OPs) in fmERG are shown. *: a-wave; †: b-wave. ON = stimulus onset.

MDRF and the mean INL and ONL+OPL thicknesses were calculated, and the correlations of MDRF with the INL and ONL+OPL thicknesses were examined.

Surgical Procedure

The indication for ERM surgery was determined on the basis of decreased visual acuity (less than 20/20) or a complaint of metamorphopsia. All surgeries were performed using a 25-gauge microincision vitrectomy system (Constellation; Alcon Laboratories, Inc) by 1 of 2 surgeons (Y.M. and I.T.). After core vitrectomy, ERM was removed as much as possible. Internal limiting membrane was removed after staining with 0.25 mg/mL Brilliant Blue G solution (Coomassie BBG 250; Sigma-Aldrich). At a minimum, the minimum area of ILM peeling was larger than the parafoveal area and selected at the discretion of the surgeon.[12,18,19]

Quantitative Analysis of α-Smooth Muscle Actin Gene Expression Using Real-Time Reverse Transcription Polymerase Chain Reaction

To quantitatively evaluate the gene expression of α-smooth muscle actin (α-SMA) in surgically removed ERM specimens, real-time reverse transcription polymerase chain reaction was performed according to the methods of Shiode et al,[25] using TaqMan primers (α-SMA [ACTA2], Hs00426835_g1; glyceraldehyde 3-phosphate dehydrogenase, Hs02786624_g1) (Thermo Fisher Scientific). The relative expression of ACTA2 was calculated using the ΔΔCt

Table 1. Comparisons of the Amplitudes in Focal Macular Electroretinogram Performed for Patients With Idiopathic Epiretinal Membrane

	Affected Eyes (μV)	Fellow Eyes (μV)	Relative Amplitudes (%)
a-wave	1.13 ± 0.13	1.43 ± 0.12	85 ± 13
b-wave	2.80 ± 0.19*	3.72 ± 0.33	81 ± 7
OPs	1.16 ± 0.12*	1.93 ± 0.17	64 ± 6

OPs = oscillatory potentials.
Values are expressed as mean ± standard error. Significance is in comparison to the normal fellow eyes; paired *t*-test.
*$P < 0.05$.

method, with glyceraldehyde 3-phosphate dehydrogenase used as an internal control.

Immunohistochemical Analysis of α-SMA Expression in ERM

Immunohistochemical staining was performed by partially modifying a previously described method.[25] For immunohistochemical staining, anti-α-SMA antibody (1:200, Cat. no. A5228; Sigma-Aldrich) and Alexa Fluor 488-conjugated goat anti-mouse IgG (1:500, Cat. no. A-11029; Thermo Fisher Scientific) were used as primary and secondary antibodies, respectively. Cells were stained with 4',6-diamidino-2-phenylindole (1:500, Thermo Fisher Scientific).

Statistical Analysis

All statistical analyses were performed using SPSS version 25.0.0.0 (IBM Corporation). A paired t-test was used to compare the amplitudes of a-waves, b-waves, and OPs in ERM and normal fellow eyes. Spearman's rank correlation test was used to analyze the following relationships: MDRF and relative amplitudes of b-waves and OPs; MDRF and the mean INL and ONL+OPL thicknesses; progression rate for MDRF and progression rate for the mean INL and mean ONL+OPL thicknesses; MDRF and superior, inferior, nasal, and temporal INL and ONL+OPL thicknesses; and MDRF and relative expression of α-SMA. The Kruskal–Wallis test was used to compare superior, inferior, nasal, and temporal INL and ONL+OPL thicknesses, respectively. Unless otherwise noted, the data are shown as mean ± standard error for the amplitudes and implicit times and mean ± standard deviation for the other values. A *P*-value of < 0.05 was considered statistically significant.

Results

Relationships Between MDRF and Relative Amplitudes of Each Focal Macular ERG Component

We examined the relationships between MDRF and the amplitudes of a-waves, b-waves, and OPs for 13 eyes of 13 patients (mean age: 69.8 ± 5.5 years; 8 men and 5 women). Representative ERGs for a normal fellow eye and an ERM eye are shown in Figure 3A, B. First, the amplitude of each component was compared with that for the normal fellow eye. There was no significant difference in the amplitude of a-waves between ERM eyes and normal fellow eyes (a-waves: fellow eye, 1.43 ± 0.12 μV; affected eye, 1.13 ± 0.13 μV; $P = 0.092$); however, the amplitudes of b-waves and OPs were significantly smaller for ERM eyes than for normal fellow eyes (b-waves: fellow eye, 3.72 ± 0.33 μV; affected eye, 2.80 ± 0.19 μV; OPs: fellow eye, 1.93 ± 0.17 μV; affected eye, 1.16 ± 0.12 μV; $P = 0.012$ and $P = 0.001$, respectively, Table 1). There was no significant difference in the implicit time of a-waves between the ERM and normal eyes (a-waves: fellow eye, 28.2 ± 1.0 msec; affected eye, 28.1 ± 0.4 msec; $P = 0.932$; Table 2). On the other hand, the implicit time of b-waves was significantly prolonged for the ERM eyes than for the normal fellow eyes (b-wave: fellow eye, 47.2 ± 0.6 msec; affected eye, 49.4 ± 0.6 msec; $P = 0.021$). The implicit time of OP1 was not significantly different between eyes (fellow eye, 31.3 ± 0.5 msec; affected eye, 32.6 ± 0.7 msec; $P = 0.113$). On the other hand, the implicit times of OP2 and OP3 were significantly longer for the ERM eyes than for the normal fellow eyes (OP2: fellow eye, 38.2 ± 0.3 msec; affected eye, 39.7 ± 0.5 msec; $P = 0.016$; OP3: fellow eye, 45.3 ± 0.2 msec; affected eye, 47.3 ± 0.5 msec, $P = 0.002$). Because the amplitudes of b-waves and OPs were significantly decreased for ERM eyes compared with normal fellow eyes, we examined the relationship of MDRF with b-wave and OP parameters and found that MDRF was significantly correlated with the relative amplitudes of both b-waves and OPs ($r = -0.657$, $P = 0.015$; $r = -0.569$, $P = 0.042$, respectively; Fig 3C, D).

Relationships of MDRF With Mean INL and ONL+OPL Thicknesses

The relationships of MDRF with the mean INL and ONL+OPL thicknesses were examined for 166 eyes of 163 ERM patients (mean age: 69.3 ± 7.8 years, 77 men and 86 women) and found significant correlations ($r = 0.604$, $P < 0.001$; $r = 0.210$, $P = 0.007$, respectively; Fig 4A, B).

Relationships Between the Progression Rate for MDRF and the Progression Rates for the Mean INL and ONL+OPL Thicknesses

For 32 eyes of 27 ERM patients who were followed up without surgery (mean age: 71.1 ± 8.6 years, 14 men and 13

Table 2. Comparisons of Implicit Times in Focal Macular Electroretinogram Performed for Patients With Idiopathic Epiretinal Membrane

	Affected Eyes (msec)	Fellow Eyes (msec)	P Value
a-wave	28.1 ± 0.4	28.2 ± 1.0	0.932
b-wave	49.4 ± 0.6	47.2 ± 0.6	0.021
OP1	32.6 ± 0.7	31.3 ± 0.5	0.113
OP2	39.7 ± 0.5	38.2 ± 0.3	0.016
OP3	47.3 ± 0.5	45.3 ± 0.2	0.002

OP = oscillatory potential.
Values are expressed as mean msec ± standard error.

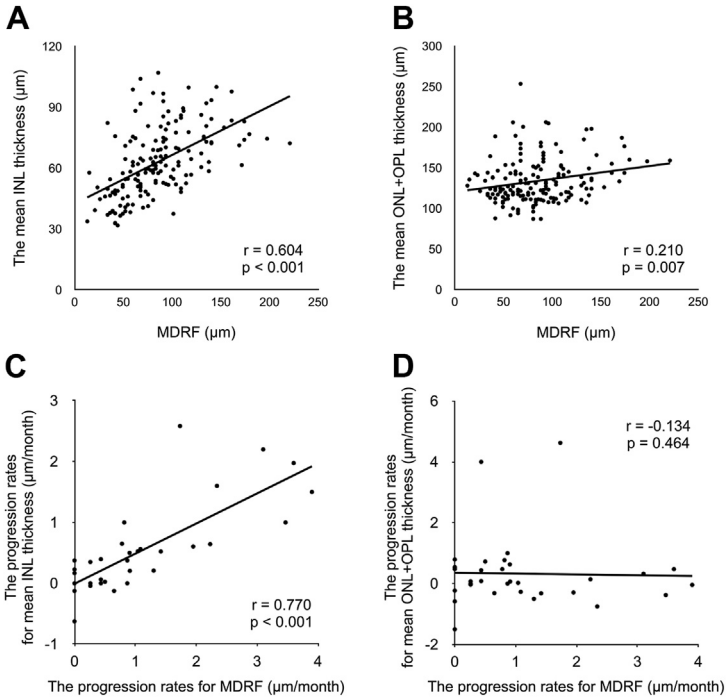

Figure 4. Relationships between the maximum depth of retinal folds within the parafovea (MDRF) and the thicknesses of the inner nuclear layer (INL) and outer nuclear layer (ONL) + outer plexiform layer (OPL) in patients with epiretinal membrane. **A, B,** The relationships between MDRF and the mean INL and ONL+OPL thicknesses are shown. **C, D,** The relationships between the MDRF progression rate and the progression rates for the mean INL and ONL+OPL thicknesses are shown.

women), we examined the relationships between the progression rate for MDRF and the progression rates for the mean INL and ONL+OPL thicknesses. The mean follow-up period was 8.8 ± 2.5 months, and the progression rates for MDRF, the mean INL thickness, and the mean ONL+OPL thickness were 1.1 ± 1.1, 0.5 ± 0.7, and 0.3 ± 1.2 μm/month, respectively. The progression rate for MDRF significantly correlated with the progression rate for the mean INL thickness ($r = 0.770$, $P < 0.001$). On the other hand, there was no significant correlation between the progression rate for MDRF and the progression rate for the mean ONL+OPL thickness ($r = -0.134$, $P = 0.464$; Fig 4C, D).

Relationship Between MDRF Localization and the INL Thickness in Each Region of the ETDRS Chart

The relationship between MDRF localization and the INL thickness at 1000 μm away from the fovea in each region of the ETDRS chart was examined for 166 eyes of 163 patients with ERM (mean age: 69.3 ± 7.8 years, 77 men and 86 women). The results showed that MDRF was localized in the superior, inferior, nasal, and temporal regions of the ETDRS chart in 48, 46, 34, and 32 eyes, respectively. In 6 eyes, MDRF was located in the central area of the ETDRS chart (i.e., within a 1-mm-diameter circle centered on the fovea). In cases where MDRF was localized in the superior, inferior, and nasal areas, the area where MDRF was localized coincided with the area with the thickest INL (Fig 5A–C). In cases with MDRF localized in the temporal area, the INL thickness in the temporal area (71.9 ± 18.0 μm) was significantly greater than that in the nasal and inferior areas (56.0 ± 18.2 μm and 54.6 ± 20.1 μm, respectively; $P < 0.05$ for both) and tended to be greater than the INL thickness in the superior area (62.9 ± 28.2 μm; $P = 0.051$; Fig 5D).

The relationship between MDRF and the INL thickness in each region of the ETDRS chart was examined (Table 3). The MDRF showed a significant correlation with the INL thickness in areas where MDRF was localized as well as other areas. The strongest correlation between MDRF and the INL thickness was observed in areas where MDRF was localized, with the exception of the temporal area (Table 3). On the other hand, there was no significant correlation between the localization of MDRF and the ONL+OPL thickness in areas where MDRF was localized (Fig S6 and Table S4).

Relationship Between MDRF and Expression of α-SMA in ERM

We performed real-time reverse transcription polymerase chain reaction using ERM specimens collected from 21 eyes (mean age: 70.5 ± 5.9, 11 men and 10 women). The results showed that the relative expression of α-SMA significantly correlated with MDRF ($r = 0.555$, $P = 0.009$; Fig 7A). This result was consistent with the results of immunohistochemical staining of ERM with α-SMA antibodies. The results of staining in 2 representative cases are shown in Figure 7B.

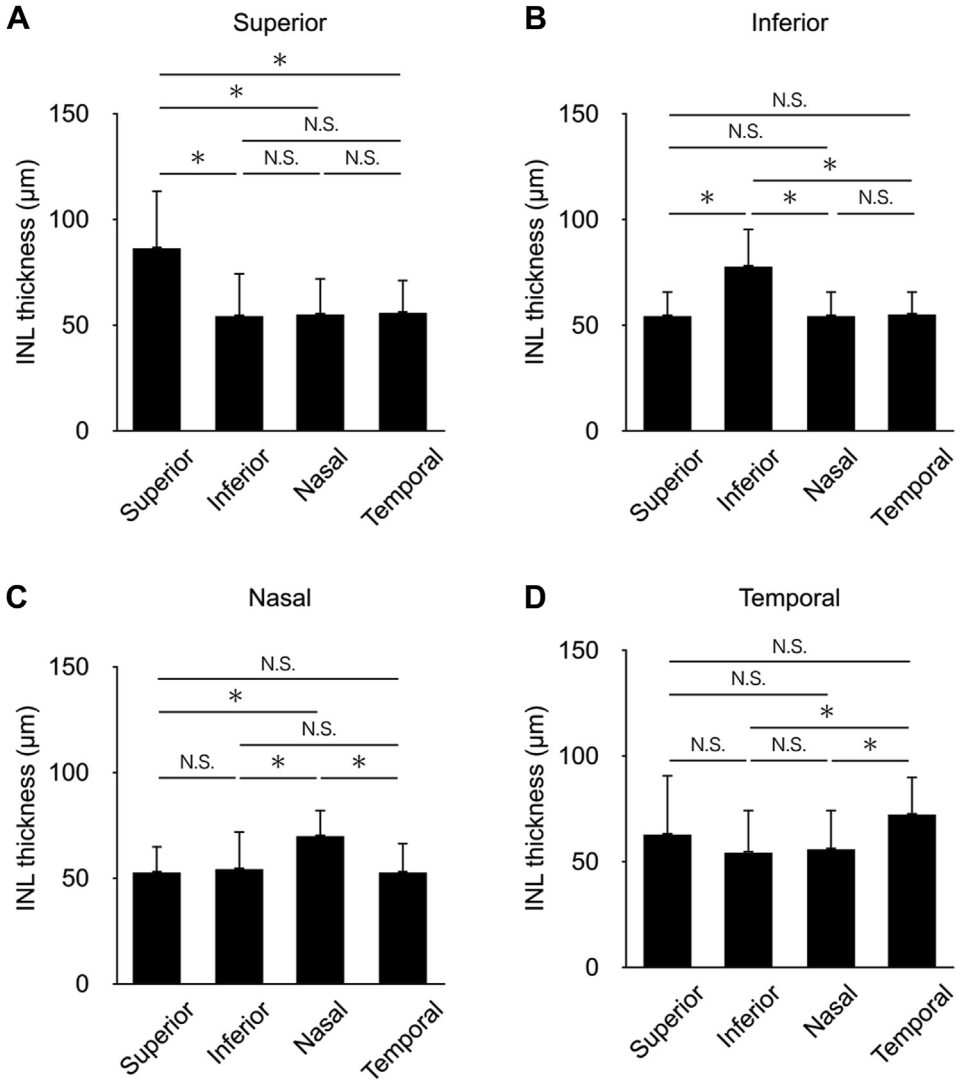

Figure 5. Comparisons of the inner nuclear layer (INL) thickness in each area after stratification of cases according to localization of the maximum depth of retinal folds (**A,** superior, **B,** inferior, **C,** nasal, and **D,** temporal) among patients with epiretinal membrane. *$P < 0.05$; N.S. = not significant.

Table 3. Correlations Between the Maximum Depth of Retinal Folds and Retinal Microstructure in Patients With Epiretinal Membrane

Localization of the Deepest Retinal Fold	INL Thickness			
	Superior	*Inferior*	*Nasal*	*Temporal*
Superior	r = 0.671	r = 0.336	r = 0.457	r = 0.451
	$P < 0.001$	$P = 0.019$	$P = 0.001$	$P = 0.001$
Inferior	r = 0.428	r = 0.598	r = 0.362	r = 0.389
	$P = 0.003$	$P < 0.001$	$P = 0.013$	$P = 0.008$
Nasal	r = 0.431	r = 0.427	r = 0.737	r = 0.266
	$P = 0.011$	$P = 0.012$	$P < 0.001$	$P = 0.128$
Temporal	r = 0.786	r = 0.653	r = 0.606	r = 0.678
	$P < 0.001$	$P < 0.001$	$P < 0.001$	$P < 0.001$

INL = inner nuclear layer.

Discussion

In this study, we found that electrophysiological dysfunction and structural changes in the inner retinal layer occur in ERM patients in a traction force-dependent manner. The following 3 results support this conclusion. First, MDRF, which is the biomarker for the retinal traction force due to ERM, was correlated with the degree of electrophysiological dysfunction of the inner retina. Second, the degree, localization, and progression rate of MDRF were correlated with the degree of thickening, localization, and progression rate of INL. Third, MDRF was associated with the expression level of α-SMA in surgically excised ERM specimens.

The results of our focal macular ERG study showed that MDRF significantly correlated with the degree of impaired ERG response of the inner retina. The amplitudes of both

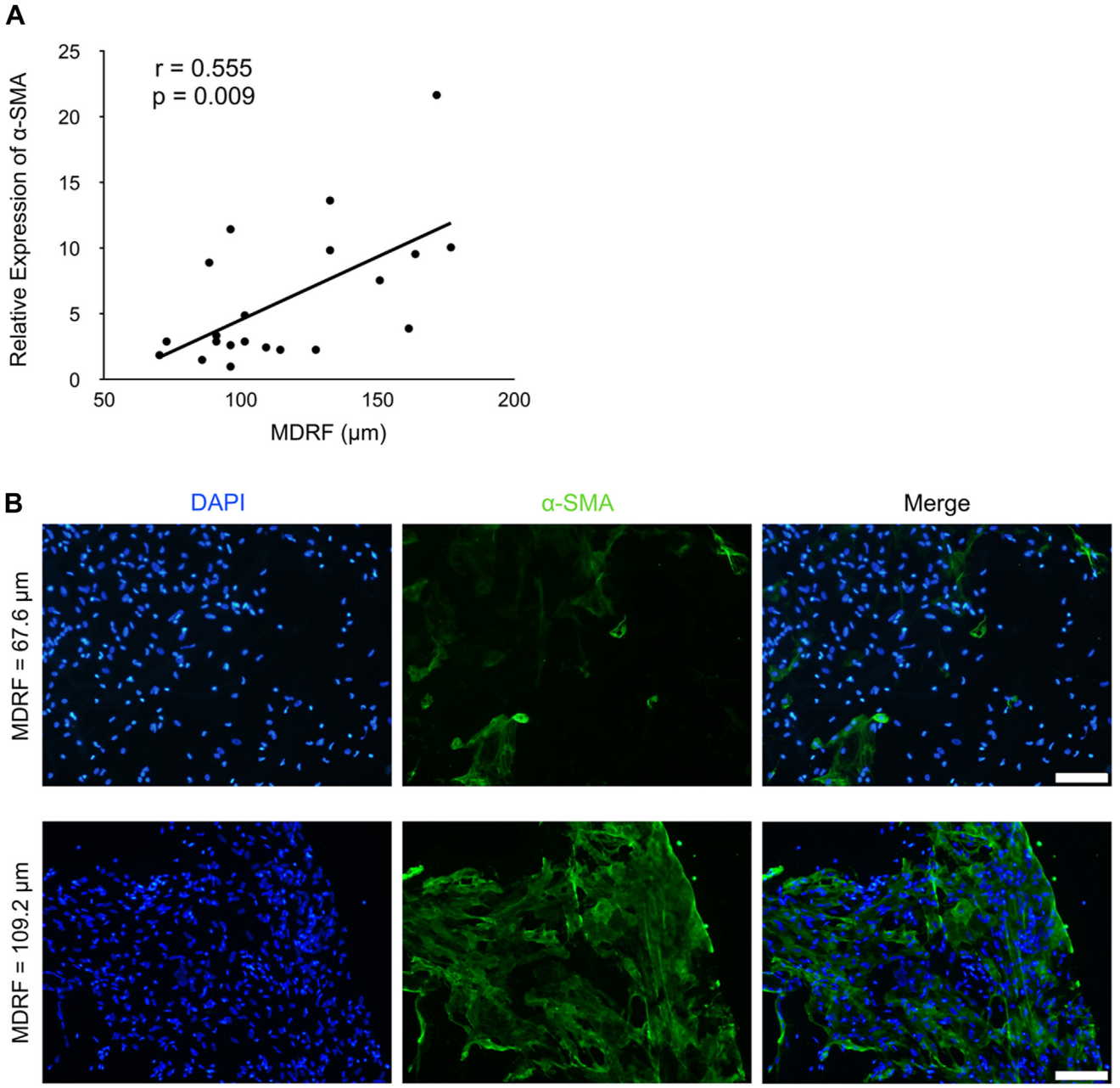

Figure 7. Relationship between the maximum depth of retinal folds (MDRF) and α-smooth muscle actin (α-SMA) expression in surgically removed epiretinal membrane (ERM) specimens. **A,** The relationship between MDRF and the relative expression of the α-SMA gene in ERM specimens is shown. **B,** The results of immunohistochemical staining in 2 representative cases are shown. Scale bar: 50 μm. DAPI = 4',6-diamidino-2-phenylindole.

b-waves and OPs significantly decreased in eyes with ERM, as in previous reports.[22–24] Several studies have suggested that the b-wave originates mainly from the on-bipolar cells,[26–28] and the OPs originate from the amacrine cells.[29–31] Furthermore, MDRF was negatively and significantly correlated with the relative amplitudes of both b-waves and OPs. Because MDRF is an objective and quantitative biomarker that reflects the severity of ERM-induced retinal traction,[12,16–20] these results indicate that ERM-induced retinal traction preferentially impairs INL in a retinal traction force-dependent manner.

Based on the focal macular ERG results, we focused on the structural changes in the inner retinal layers, especially INL, due to ERM traction. To date, it has been reported that INL thickens in patients with ERM,[6,7,13,14] and that the degree of INL thickening is associated with the degree of visual dysfunction, such as reduced visual acuity[6,7,14] and metamorphopsia.[6,7,13] However, the relationship between INL thickening and retinal traction force by ERM remained unknown. In the present study, MDRF and its localization on the ETDRS chart were significantly associated with the degree of INL thickening (Figs 4A

and 5) and its localization (Table 3). Furthermore, the progression rate for MDRF in the natural course was significantly correlated with the progression rate for the INL thickness (Fig 4C). These results indicate that INL thickening is induced by ERM in a retinal traction force-dependent manner.

As opposed to the association with the inner retinal thickness, the association between MDRF and changes in the thickness of the outer retina, specifically ONL+OPL, was not apparent in this study. Although a significant correlation between MDRF and the ONL+OPL thickness was found (Fig 4B), there were no significant correlations between the progression rates for MDRF and the ONL+OPL thickness over time and between the localization of MDRF and ONL+OPL thickening (Table S4 and Fig 4D). These results did not support the previous finding of ONL+OPL thickening in ERM cases.[6,7,13] Okamoto et al[7] reported that although metamorphopsia was associated with INL in ERM, no association was found between metamorphopsia and the ONL+OPL thickness. Considering the results of this study and the study of Okamoto et al, the role of changes in ONL+OPL in the pathogenesis of ERM and the related visual disturbance may not be as important as the role of changes in INL. Possible reasons for the differences in the effects of ERM-related retinal traction between INL and ONL+OPL include the following: (1) differences in the distance from the retinal surface to each retinal layer and (2) differences in the cells that make up each layer of the retina. Further analysis is needed to determine the mechanism underlying the preferential effects of ERM-related retinal traction on INL.

We found that MDRF correlated with the expression level of α-SMA, 1 of the major factors causing contractility of ERM, in surgically excised ERM specimens. The major components of idiopathic ERM include glial cells,[32,33] hyalocytes,[32,34] and myofibroblasts.[33] It is well known that glial cells[33] and hyalocytes[34,35] transform into myofibroblasts, which express α-SMA.[33,36] We previously reported that MDRF is a biomarker for estimating the retinal traction force due to ERM based on the physical properties of membranous structures under compressive stress.[37−39] However, the molecular background of the relationship between MDRF and the retinal traction force due to ERM is unknown.[12,16−20] The present study showed that MDRF correlates with the expression level of α-SMA in ERM, thus supporting the validity of MDRF as an indicator of the retinal traction force due to ERM from a molecular perspective. In the future, it will be necessary to investigate the relationship between MDRF and the expression of other factors involved in ERM contractility, such as tumor growth factor-β2 and other cytokines.[33,35,36]

The limitations of this study include its retrospective nature, the small sample size, and the relatively short follow-up period. Furthermore, we did not examine the relationships between MDRF and ERM symptoms other than metamorphopsia, such as aniseikonia and contrast sensitivity.[5,10,40] Moreover, factors other than MDRF, such as retinal fold parameters (ie, the number, location, and duration of folds), components of ERM, and physical properties of the retina owing to the patient's age, may be involved in the visual impairment caused by ERM. Therefore, further investigation is needed.

In conclusion, this study demonstrated that MDRF was significantly correlated with a decline in the electrophysiological function of the inner retinal layer, thickening of INL, and expression of α-SMA in eyes with ERM. These results suggest that ERM preferentially impairs the inner retinal layer in a retinal traction force-dependent manner.

Acknowledgments

The authors thank Kumiko Kikuchi and Shiori Ikeda for technical laboratory assistance.

Footnotes and Disclosures

Originally received: January 4, 2023.
Final revision: April 7, 2023.
Accepted: April 7, 2023.
Available online: April 15, 2023. Manuscript no. XOPS-D-23-00003.

[1] Department of Ophthalmology, Graduate School of Medicine, Dentistry and Pharmaceutical Sciences, Okayama University, Okayama City, Okayama, Japan.

[2] Takasu Eye Clinic, Okayama City, Okayama, Japan.

[3] Department of Ophthalmology, Fujita Health University Bantane Hospital, Nagoya City, Aichi, Japan.

Disclosures:

All authors have completed and submitted the ICMJE disclosures form.

The authors made the following disclosures:

No conflicting relationship exists for any author.

This study was supported by grants from JSPS KAKENHI [grant numbers 21K16872 and 21K20971].

HUMAN SUBJECTS: Human subjects were used in this study. The study protocol was approved by the Ethics Committee of Okayama University Hospital, Okayama, Japan (K2205-010 and K1608-014) and adhered to the tenets of the Declaration of Helsinki. Each patient was informed about the nature and possible consequences of the study and provided written informed consent for participation. No animals were used in this study.

Author Contributions:

Conception and design: Y. Kanzaki, Matoba, Doi, Tanikawa, Morizane

Data collection: Y. Kanzaki, Matoba, Morita, S. Kanzaki, Takasu

Analysis and interpretation: Y. Kanzaki, Matoba, Kimura, Hosokawa, Doi, Tanikawa, Morizane

Obtained funding: N/A

Overall responsibility: Y. Kanzaki, Matoba, Shiode, Morita, S. Kanzaki, Takasu, Tanikawa, Morizane

Abbreviations and Acronyms:
ERG = electroretinogram; **ERM** = epiretinal membrane; **ILM** = internal limiting membrane; **INL** = inner nuclear layer; **MDRF** = maximum depth of retinal folds; **ONL** = outer nuclear layer; **OPL** = outer plexiform layer; **OPs** = oscillatory potentials; **α-SMA** = α-smooth muscle actin.

Keywords:
Epiretinal membrane, En face OCT, Retinal traction force, Inner nuclear layer, Focal macular electroretinogram.

Correspondence:
Yuki Morizane, MD, PhD, Department of Ophthalmology, Graduate School of Medicine, Dentistry and Pharmaceutical Sciences, Okayama University, 2-5-1 Shikata-cho Kita-ku, Okayama City, Okayama 700-8558, Japan. E-mail: moriza-y@okayama-u.ac.jp.

References

1. Fraser-Bell S, Guzowski M, Rochtchina E, et al. Five-year cumulative incidence and progression of epiretinal membranes: the Blue Mountains Eye study. *Ophthalmology*. 2003;110:34−40.
2. Bu SC, Kuijer R, Li XR, et al. Idiopathic epiretinal membrane. *Retina*. 2014;34:2317−2335.
3. Matoba R, Morizane Y. Surgical treatment of epiretinal membrane. *Acta Med Okayama*. 2021;75:403−413.
4. Kinoshita T, Imaizumi H, Okushiba U, et al. Time course of changes in metamorphopsia, visual acuity, and OCT parameters after successful epiretinal membrane surgery. *Invest Ophthalmol Vis Sci*. 2012;53:3592−3597.
5. Okamoto F, Okamoto Y, Hiraoka T, Oshika T. Effect of vitrectomy for epiretinal membrane on visual function and vision-related quality of life. *Am J Ophthalmol*. 2009;147:869−874, 874.e1.
6. Okamoto F, Sugiura Y, Okamoto Y, et al. Associations between metamorphopsia and foveal microstructure in patients with epiretinal membrane. *Invest Ophthalmol Vis Sci*. 2012;53:6770−6775.
7. Okamoto F, Sugiura Y, Okamoto Y, et al. Inner nuclear layer thickness as a prognostic factor for metamorphopsia after epiretinal membrane surgery. *Retina*. 2015;35:2107−2114.
8. Arimura E, Matsumoto C, Nomoto H, et al. Correlations between M-CHARTS and PHP findings and subjective perception of metamorphopsia in patients with macular diseases. *Invest Ophthalmol Vis Sci*. 2011;52:128−135.
9. Arimura E, Matsumoto C, Okuyama S, et al. Retinal contraction and metamorphopsia scores in eyes with idiopathic epiretinal membrane. *Invest Ophthalmol Vis Sci*. 2005;46:2961−2966.
10. Tanikawa A, Shimada Y, Horiguchi M. Comparison of visual acuity, metamorphopsia, and aniseikonia in patients with an idiopathic epiretinal membrane. *Jpn J Ophthalmol*. 2018;62:280−285.
11. Amsler M. Earliest symptoms of diseases of the macula. *Br J Ophthalmol*. 1953;37:521−537.
12. Hirano M, Morizane Y, Kanzaki Y, et al. En face image−based analysis of retinal traction caused by epiretinal membrane and its relationship with visual functions. *Retina*. 2020;40:1262−1271.
13. Ichikawa Y, Imamura Y, Ishida M. Inner nuclear layer thickness, a biomarker of metamorphopsia in epiretinal membrane, correlates with tangential retinal displacement. *Am J Ophthalmol*. 2018;193:20−27.
14. Govetto A, Lalane RA, Sarraf D, et al. Insights into epiretinal membranes: presence of ectopic inner foveal layers and a new optical coherence tomography staging scheme. *Am J Ophthalmol*. 2017;175:99−113.
15. Morizane Y, Kanzaki Y, Doi S. Macular epiretinal membrane surgery. In: Albert D, Miller J, Azar D, Young LH, eds. *Albert and Jakobiec's Principles and Practice of Ophthalmology*. Cham: Springer; 2021:1−27.
16. Hirano M, Morizane Y, Kimura S, et al. Assessment of lamellar macular hole and macular pseudohole with a combination of en face and radial B-scan optical coherence tomography imaging. *Am J Ophthalmol*. 2018;188:29−40.
17. Matoba R, Kanzaki Y, Doi S, et al. Assessment of epiretinal membrane formation using en face optical coherence tomography after rhegmatogenous retinal detachment repair. *Graefes Arch Clin Exp Ophthalmol*. 2021;259:2503−2512.
18. Kanzaki S, Kanzaki Y, Doi S, et al. En face image-based analysis of epiretinal membrane formation after surgery for idiopathic epiretinal membrane. *Ophthalmol Retina*. 2021;5:815−823.
19. Kanzaki Y, Doi S, Matoba R, et al. Objective and quantitative estimation of the optimal timing for epiretinal membrane surgery on the basis of metamorphopsia. *Retina*. 2022;42:704−711.
20. Fujiwara A, Kanzaki Y, Kimura S, et al. En face image-based classification of diabetic macular edema using swept source optical coherence tomography. *Sci Rep*. 2021;11:1−14.
21. Matsumoto C, Arimura E, Okuyama S, et al. Quantification of metamorphopsia in patients with epiretinal membranes. *Invest Ophthalmol Vis Sci*. 2003;44:4012−4016.
22. Tanikawa A, Horiguchi M, Kondo M, et al. Abnormal focal macular electroretinograms in eyes with idiopathic epimacular membrane. *Am J Ophthalmol*. 1999;127:559−564.
23. Hibi N, Ueno S, Ito Y, et al. Relationship between retinal layer thickness and focal macular electroretinogram components after epiretinal membrane surgery. *Invest Ophthalmol Vis Sci*. 2013;54:7207−7214.
24. Niwa T, Terasaki H, Kondo M, et al. Function and morphology of macula before and after removal of idiopathic epiretinal membrane. *Invest Ophthalmol Vis Sci*. 2003;44:1652−1656.
25. Shiode Y, Morizane Y, Matoba R, et al. The role of inverted internal limiting membrane flap in macular hole closure. *Invest Ophthalmol Vis Sci*. 2017;58:4847−4855.
26. Knapp AG, Schiller PH. The contribution of on-bipolar cells to the electroretinogram of rabbits and monkeys. A study using 2-amino-4-phosphonobutyrate (APB). *Vis Res*. 1984;24:1841−1846.
27. Sieving PA, Murayama K, Naarendorp F. Push-pull model of the primate photopic electroretinogram: a role for hyperpolarizing neurons in shaping the b-wave. *Vis Neurosci*. 1994;11:519−532.
28. Kondo M, Ueno S, Piao CH, et al. Comparison of focal macular cone ERGs in complete-type congenital stationary night blindness and APB-treated monkeys. *Vis Res*. 2008;48:273−280.
29. Korol S, Leuenberger PM, Englert U, Babel J. In vivo effects of glycine on retinal ultrastructure and averaged electroretinogram. *Brain Res*. 1975;97:235−251.
30. Nakatsuka K, Hamasaki DI. Destruction of the indoleamine-accumulating amacrine cells alters the ERG of rabbits. *Investig Ophthalmol Vis Sci*. 1985;26:1109−1116.
31. Wachtmeister L. Oscillatory potentials in the retina: what do they reveal. *Prog Retin Eye Res*. 1998;17:485−521.
32. Schumann RG, Eibl KH, Zhao F, et al. Immunocytochemical and ultrastructural evidence of glial cells and hyalocytes in internal limiting membrane specimens of idiopathic macular holes. *Invest Ophthalmol Vis Sci*. 2011;52:7822−7834.

33. Bu SC, Kuijer R, van der Worp RJ, et al. Immunohistochemical evaluation of idiopathic epiretinal membranes and in vitro studies on the effect of TGF-β on Müller cells. *Investig Ophthalmol Vis Sci*. 2015;56:6506−6514.
34. Kohno R, Hata Y, Kawahara S, et al. Possible contribution of hyalocytes to idiopathic epiretinal membrane formation and its contraction. *Br J Ophthalmol*. 2009;93:1020−1026.
35. Joshi M, Agrawal S, Christoforidis JB. Inflammatory mechanisms of idiopathic epiretinal membrane formation. *Mediators Inflamm*. 2013;2013:192582.
36. Tsotridou E, Loukovitis E, Zapsalis K, et al. A review of last decade developments on epiretinal membrane pathogenesis. *Med Hypothesis Discov Innov Ophthalmol*. 2020;9:91−110.
37. Roddeman DG, Drukker J, Oomens CWJ, Janssen JD. The wrinkling of thin membranes: part I—theory. *J Appl Mech*. 1987;54:884−887.
38. Roddeman DG, Drukker J, Oomens CW, Janssen JD. The wrinkling of thin membranes: part II—numerical analysis. *J Appl Mech*. 1987;54:888−892.
39. Miyazaki Y. Wrinkle/slack model and finite element dynamics of membrane. *Int J Numer Methods Eng*. 2006;66:1179−1209.
40. Sugiura Y, Okamoto F, Okamoto Y, et al. Contrast sensitivity and foveal microstructure following vitrectomy for epiretinal membrane. *Invest Ophthalmol Vis Sci*. 2014;55:7594−7600.